X-552-70-289

PREPRINT

NASA TM X- 65317

LUNAR GRAVITY MODELS FOR IMPROVED APOLLO ORBIT COMPUTATION

JAMES P. MURPHY

THEODORE L. FELSENTREGER

CARL A. WAGNER

JAMES W. RYAN

JULY 1970

GSFC

GODDARD SPACE FLIGHT CENTER

GREENBELT, MARYLAND

X-552-70-289
PREPRINT

LUNAR GRAVITY MODELS FOR IMPROVED APOLLO ORBIT COMPUTATION

James P. Murphy
Theodore L. Felsentreger
Carl A. Wagner
Mission Trajectory Determination Branch
Mission and Trajectory Analysis Division

James W. Ryan
Data Evaluation Branch
Manned Flight Planning and Analysis Division

July 1970

GODDARD SPACE FLIGHT CENTER
Greenbelt, Maryland

ABSTRACT

Three possible modifications of the operational lunar gravity model for Apollo missions are presented. One of these is recommended for use in future Apollo missions. This field, designated ML1.1, consists of the current operational model (L1) plus the following values for the (4,1) harmonics: $C_{41} = -.1284 \times 10^{-4}$ and $S_{41} = .1590 \times 10^{-4}$. The main benefit to be derived from the use of this model lies in its capability to predict the inclination and inertial node for all the Apollo orbits accurately. The current L1 model fails to do this, especially for the low inclination cases. The (4,1) values were obtained by considering classical elements from Apollos 8, 10, 11, and 12 as observables in a least squares gravity retrieval program. The ML1.1 model performed as well or better than did the L1 field in predicting the trajectories for Apollo and Lunar Orbiter spacecraft. The tracking data were fit just as well, also. The desirable properties of the L1 model are all preserved with the ML1.1 model.

CONTENTS

LUNAR GRAVITY MODELS FOR IMPROVED APOLLO ORBIT COMPUTATION

James P. Murphy, Theodore L. Felsentreger
Carl A. Wagner and James W. Ryan
Goddard Space Flight Center

INTRODUCTION

The search for a simple lunar gravitational model adequate for Apollo mission orbit prediction has been continuing ever since the discovery of unexpectedly large anomalies in the tracking data of the Lunar Orbiter spacecrafts. These anomalies indicated that the moon's gravity field was somewhat more complex than had been thought.

For the Apollo 8 mission, the first manned flight to the moon, a tri-axial gravity model derived by Jeffreys (Reference 1) was adopted both for mission control at Mission Control Center, Houston, and for operational support at Goddard Space Flight Center. However, this model proved to have rather poor orbit prediction capability for the mission, producing unacceptably large in-plane and out-of-plane errors.

A slightly larger gravity model consisting of the C_{20}, C_{22}, C_{30}, and C_{31} spherical harmonic coefficients was developed by Risdal (Reference 2) and was adopted for operational use in the Apollo 10 and 11 missions. This model was derived from a study of the long-period variations in the orbital elements of the Lunar Orbiters, and was designated the "R2" model. While the R2 model provided improved orbit prediction capability, it still produced rather large downtrack errors and could not accurately predict orbit plane variations.

An adjustment to the R2 model was developed by Compton and Tolson from an analysis of Apollo 8 data (Reference 3), and served to reduce downtrack errors significantly for Apollo 8. This model, termed the L1 model, consists of the R2 field plus a value for the C_{33} coefficient. While having improved orbit prediction capability, the L1 model still failed to predict orbit plane variations (i.e., it could not adequately model the evolution of the inclination and longitude of ascending node).

This paper presents the results of a study designed to derive a simple lunar gravity model superior to the L1 model in Apollo orbit prediction capability, with the particular property of being able to model inclination and longitude of ascending node histories. For this study, the data used were classical orbital elements at approximately one-orbit intervals for the Apollo 8, 10, 11, and 12 missions. The Lagrange Planetary Equations were numerically integrated to provide a reference trajectory, and the appropriate spherical harmonic coefficients were solved for by weighted least squares. A more detailed description of the method used and the data sets chosen follows in succeeding sections.

The previous operational Apollo lunar gravity models (i.e., the tri-axial, R2, and L1 models) appear in Table 1.

DATA

The basic data used in the analysis consists of classical orbital elements for the Apollo 8, 10, 11, and 12 Command and Service Modules (CSM) as they orbited the moon. Each set of elements resulted from a one orbit solution for spacecraft position and velocity using Doppler data. Since, in each mission, the CSM was necessarily subjected to many orbit changes due to maneuvers, the data were divided into eight data sets, or "arcs," during each of which the spacecraft was free of such perturbations. A summary of these arcs indicating the "free flight" periods and orbit numbers involved is given in Table 2.

The orbital elements themselves for each arc, along with the Modified Julian Date (MJD) for each set of elements, are listed in Table 3. In the table,

a = semi-major axis (moon radii)

e = eccentricity

i = angle of inclination to lunar equator (degrees)

ω = argument of perilune (degrees)

N = inertial longitude of ascending node (degrees)

M = mean anomaly (degrees),

where the mean radius of the moon was taken to be 1738.09 km. For each arc, the "inertial" longitude of ascending node is the selenographic node less the mean rotation of the moon, referred to the first time point in the arc. The reason for listing the inertial nodes rather than the selenographic nodes will become clear in a later section when the data actually used as observables are discussed.

The elements for Apollos 8, 10, and 11 were taken from Reference 4, and are tabulated at perilune (i.e., mean anomaly = 0). The Apollo 12 elements were determined at GSFC, and were obtained from Reference 5—these are tabulated very near perilune. All the elements are selenographic with the exception, as noted previously, of the inertial node.

LUNAR DISTURBING POTENTIAL

The universally recommended spherical harmonic expansion for the gravitational potential at a point with spherical coordinates (r, ϕ, λ) in a rotating coordinate system with origin at the center of a primary body is (see Reference 6)

$$U = \frac{\mu}{r}\left\{1 + \sum_{\ell=2}^{\infty}\sum_{m=0}^{\ell}\left(\frac{a_m}{r}\right)^{\ell} P_{\ell m}(\sin\phi)\left[C_{\ell m}\cos m\lambda + S_{\ell m}\sin m\lambda\right]\right\}.$$

If the moon is the primary body, then

μ = gravitational constant of the moon = 4902.778 km^3/sec^2

r = distance from the center of the moon

ϕ = selenographic latitude

λ = selenographic longitude

a_m = radius of the moon = 1738.09 km

$P_{\ell m}(\sin\phi)$ = associated Legendre function of degree ℓ and order m

$C_{\ell m}$, $S_{\ell m}$ = unnormalized spherical harmonic coefficients of degree ℓ and order m.

The *disturbing potential* R is equal to the potential U minus the central force term, or

$$R = U - \frac{\mu}{r},$$

which can be written in terms of the classical orbital elements mentioned previously. However, since the spacecraft orbit data resulted from one-orbit solutions, it is unnecessary to consider terms involving mean anomaly in R. Furthermore, in this study no terms involving spherical harmonic coefficients of higher degree than four were considered. Therefore, the truncated expression for R in terms of classical orbital elements is

$$R = \frac{\mu a_m^2\left(3\sin^2 i - 2\right)}{4a^3\left(1-e^2\right)^{3/2}} C_{20}$$

$$+ \frac{3\mu a_m^2 \sin^2 i}{2a^3\left(1-e^2\right)^{3/2}}\left[C_{22}\cos 2\Omega + S_{22}\sin 2\Omega\right]$$

$$+ \frac{3\mu a_m^3 e \sin i\left(5\sin^2 i - 4\right)}{4a^4\left(1-e^2\right)^{5/2}} C_{30}\sin\omega$$

$$\frac{3\mu a_m^3 e}{16 a^4\left(1-e^2\right)^{5/2}}\left\{\left[5\sin^2 i(1+3\cos i) - 4(1+\cos i)\right]\left[C_{31}\cos(\omega+\Omega) + S_{31}\sin(\omega+\Omega)\right]\right.$$

$$\left. + \left[5\sin^2 i(1-3\cos i) - 4(1-\cos i)\right]\left[C_{31}\cos(\omega-\Omega) - S_{31}\sin(\omega-\Omega)\right]\right\}$$

$$+\frac{15\,\mu\, a_m^3\, e \sin i}{8\, a^4 \left(1-e^2\right)^{5/2}} \Big\{\left(1-2\cos i-3\cos^2 i\right)\left[C_{32}\sin(\omega+2\Omega)-S_{32}\cos(\omega+2\Omega)\right]$$

$$+\left(1+2\cos i-3\cos^2 i\right)\left[C_{32}\sin(\omega-2\Omega)+S_{32}\cos(\omega-2\Omega)\right]\Big\}$$

$$+\frac{45\,\mu\, a_m^3\, e \sin^2 i}{8\, a^4 \left(1-e^2\right)^{5/2}} \Big\{(1+\cos i)\left[C_{33}\cos(\omega+3\Omega)+S_{33}\sin(\omega+3\Omega)\right]$$

$$+(1-\cos i)\left[C_{33}\cos(\omega-3\Omega)-S_{33}\sin(\omega-3\Omega)\right]\Big\}$$

$$+\frac{3\,\mu\, a_m^4}{128\, a^5 \left(1-e^2\right)^{7/2}}\, C_{40}\, \Big\{\left(2+3e^2\right)\left(8-40\sin^2 i+35\sin^4 i\right)+10\, e^2 \sin^2 i\left(6-7\sin^2 i\right)\cos 2\omega\Big\}$$

$$+\frac{15\,\mu\, a_m^4 \sin i}{64\, a^5 \left(1-e^2\right)^{7/2}} \Big\{e^2\left[7\sin^2 i(1+2\cos i)-6(1+\cos i)\right]\left[C_{41}\sin(2\omega+\Omega)-S_{41}\cos(2\omega+\Omega)\right]$$

$$+2\left(2+3e^2\right)\cos i\left(4-7\sin^2 i\right)\left[C_{41}\sin\Omega-S_{41}\cos\Omega\right]$$

$$+e^2\left[7\sin^2 i(1-2\cos i)-6(1-\cos i)\right]\left[C_{41}\sin(2\omega-\Omega)+S_{41}\cos(2\omega-\Omega)\right]\Big\}$$

$$+\frac{15\,\mu\, a_m^4}{32\, a^5 \left(1-e^2\right)^{7/2}} \Big\{3e^2(1+\cos i)\left[7\sin^2 i\cos i-(1+\cos i)\right]\left[C_{42}\cos(2\omega+2\Omega)+S_{42}\sin(2\omega+2\Omega)\right]$$

$$+\left(2+3e^2\right)\sin^2 i\left(11-21\cos^2 i\right)\left[C_{42}\cos 2\Omega+S_{42}\sin 2\Omega\right]$$

$$-3e^2(1-\cos i)\left[7\sin^2 i\cos i+(1-\cos i)\right]\left[C_{42}\cos(2\omega-2\Omega)-S_{42}\sin(2\omega-2\Omega)\right]\Big\}$$

$$+\frac{315\,\mu\, a_m^4 \sin i}{32\, a^5 \left(1-e^2\right)^{7/2}} \Big\{e^2\left(1-3\cos^2 i-2\cos^3 i\right)\left[C_{43}\sin(2\omega+3\Omega)-S_{43}\cos(2\omega+3\Omega)\right]$$

$$-2\left(2+3e^2\right)\sin^2 i\cos i\left[C_{43}\sin 3\Omega-S_{43}\cos 3\Omega\right]$$

$$+e^2\left(1-3\cos^2 i+2\cos^3 i\right)\left[C_{43}\sin(2\omega-3\Omega)+S_{43}\cos(2\omega-3\Omega)\right]\Big\}$$

$$+\frac{315\,\mu\, a_m^4 \sin^2 i}{16\, a^5 \left(1-e^2\right)^{7/2}} \Big\{ e^2 (1+\cos i)^2 \left[C_{44} \cos (2\omega + 4\Omega) + S_{44} \sin (2\omega + 4\Omega)\right]$$

$$+ \left(2+3e^2\right) \sin^2 i \left[C_{44} \cos 4\Omega + S_{44} \sin 4\Omega\right]$$

$$+ e^2 (1-\cos i)^2 \left[C_{44} \cos (2\omega - 4\Omega) - S_{44} \sin (2\omega - 4\Omega)\right]\Big\} .$$

In this expression for R, the quantity Ω is the *selenographic* longitude of ascending node.

LAGRANGE PLANETARY EQUATIONS

The Lagrange Planetary Equations for classical (i.e., Keplerian) orbital elements, which may be found in many textbooks on Celestial Mechanics, are as follows:

$$\frac{da}{dt} = \frac{2\sqrt{a}}{\sqrt{\mu}} \frac{\partial F}{\partial M}$$

$$\frac{de}{dt} = \frac{1-e^2}{\sqrt{\mu a}\, e} \frac{\partial F}{\partial M} - \frac{\sqrt{1-e^2}}{\sqrt{\mu a}\, e} \frac{\partial F}{\partial \omega}$$

$$\frac{d\omega}{dt} = -\frac{\cos i}{\sqrt{\mu a\left(1-e^2\right)}\, \sin i} \frac{\partial F}{\partial i} + \frac{\sqrt{1-e^2}}{\sqrt{\mu a}\, e} \frac{\partial F}{\partial e}$$

$$\frac{di}{dt} = \frac{\cos i}{\sqrt{\mu a\left(1-e^2\right)}\, \sin i} \frac{\partial F}{\partial \omega} - \frac{1}{\sqrt{\mu a\left(1-e^2\right)}\, \sin i} \frac{\partial F}{\partial N}$$

$$\frac{dN}{dt} = \frac{1}{\sqrt{\mu a\left(1-e^2\right)}\, \sin i} \frac{\partial F}{\partial i}$$

$$\frac{dM}{dt} = -\frac{1-e^2}{\sqrt{\mu a}\, e} \frac{\partial F}{\partial e} - \frac{2\sqrt{a}}{\sqrt{\mu}} \frac{\partial F}{\partial a} ,$$

where F represents any disturbing function. For the equations, the reference coordinate system must be inertial (i.e., non-rotating); thus, for our purposes, the quantity N would be the *inertial* longitude of ascending node. The disturbing potential R defined previously will be used as the disturbing function F. Since R does not contain the mean anomaly M, the equations for da/dt and dM/dt, and that part of de/dt involving $\partial F/\partial M$, are not needed. Therefore, the equations to be considered are

$$\frac{de}{dt} = -\frac{\sqrt{1-e^2}}{\sqrt{\mu a}\, e}\frac{\partial R}{\partial \omega}$$

$$\frac{d\omega}{dt} = -\frac{\cos i}{\sqrt{\mu a\left(1-e^2\right)}\, \sin i}\frac{\partial R}{\partial i} + \frac{\sqrt{1-e^2}}{\sqrt{\mu a}\, e}\frac{\partial R}{\partial e}$$

$$\frac{di}{dt} = \frac{\cos i}{\sqrt{\mu a\left(1-e^2\right)}\, \sin i}\frac{\partial R}{\partial \omega} - \frac{1}{\sqrt{\mu a\left(1-e^2\right)}\, \sin i}\frac{\partial R}{\partial N}$$

$$\frac{dN}{dt} = \frac{1}{\sqrt{\mu a\left(1-e^2\right)}\, \sin i}\frac{\partial R}{\partial i}\,.$$

ANALYSIS

The problem now remains to determine which spherical harmonic coefficients should be solved for, and which data should be used in the solutions. As mentioned previously, it was noted that the L1 model possessed better Apollo orbit prediction capabilities than both the tri-axial and R2 models; its main shortcoming was its failure to predict orbit plane variations (i.e., variations in inclination and longitude of ascending node). As a primary "grand-rule," therefore, it was decided to seek an extension to the L1 model rather than alter any of its coefficients, with emphasis placed on inclination and node prediction.

In addition, because of restrictions imposed by such things as the size of mission operation computer programs and the gravity field capacity wired into the spacecraft computer, and the desire to keep trajectory computing time to a minimum, it was decided to consider only those spherical harmonic coefficients of degree and order four or less. It was also decided to forego solving for the fourth degree zonal harmonic (C_{40}) because zonals are best determined from secular and long period orbital element variations over considerably longer time spans than are covered by the data.

Now, the Apollo 8, 10, 11, and 12 orbits can be characterized as having relatively low eccentricities and inclinations. Since the Lagrange Planetary Equations involve divisiors of e and $\sin i$, those terms in the various partial derivatives of R not containing factors of e and $\sin i$ will provide perturbative effects enhanced by these relatively small divisors. This fact, coupled with the indication of high correlations among fourth degree coefficients from some preliminary computer runs, narrowed the choice of coefficients to be determined to the (3,2) and (4,1) harmonics. In addition, the analysis indicated that the (3,2) coefficients could best be determined from the $\dot{e}$ and $\dot{\omega}$ data, and the (4,1) coefficients from the $\dot{i}$ and $\dot{N}$ data.

To summarize, then, the principal factors and guidelines considered in selection of the spherical harmonic coefficients to be solved for and the data to be used were the following:

1. The L1 model would be held fixed.
2. No spherical harmonic coefficient with degree and order greater than four would be solved for.
3. No zonal harmonic coefficient (i.e., order = 0) would be solved for.
4. Only the (3, 2) and (4, 1) coefficients would be solved for, the former from e and ω data, and the latter from i and N data.

METHOD OF SOLUTION

As was mentioned previously, solutions for the spherical harmonic coefficients were carried out by a weighted least squares procedure, and integration of the Lagrange Planetary Equations was performed numerically. The computer program used in obtaining the solutions is called ROAD (Rapid Orbit Analysis and Determination Program), which essentially is designed to solve for common geodetic parameters and initial satellite orbital elements from the long term evolution of Kepler elements for a number of individual satellite arcs (Reference 7).

The program uses as an orbit generator the numerical integration of the Lagrange Planetary Equations. Partial derivatives of the observations (i.e., Kepler elements) with respect to solved-for parameters (spherical harmonic coefficients and initial conditions) are obtained by simultaneous numerical integration of the "variation equations." These variation equations are found in the following manner:

Let the Lagrange Planetary Equations be written as

$$\frac{de_i}{dt} = f_i\left(e_j, c_k\right),$$

where

e_i = Kepler elements ($i = 1, 2, \cdots, 6$)

c_k = spherical harmonic coefficients ($k = 1, 2, \cdots$, no. of coefficients included)

f_i = function associated with e_i.

Then, the variation equations are

$$\frac{d}{dt}\left[\frac{\partial e_i}{\partial c_k}\right] = \sum_{j=1}^{6} \frac{\partial f_i}{\partial e_j}\left[\frac{\partial e_j}{\partial c_k}\right] + \frac{\partial f_i}{\partial c_k} \qquad \begin{pmatrix} i = 1, 2, \cdots, 6 \\ k = 1, 2, \cdots, \text{no. of coefficients} \end{pmatrix}$$

$$\frac{d}{dt}\left[\frac{\partial e_i}{\partial e_{j,0}}\right] = \sum_{m=1}^{6} \frac{\partial f_i}{\partial e_m}\left[\frac{\partial e_m}{\partial e_{j,0}}\right] \qquad (j = 1, 2, \cdots, 6)$$

where

$e_{j,0}$ = initial value of e_j.

These equations are numerically integrated to obtain the observation partial derivatives $\partial e_i/\partial c_k$ and $\partial e_i/\partial e_{j,0}$ which are needed for the first order differential corrections. The observation partials and residuals are combined to form the observation equations. An estimate of the accuracy of each observation quantity is used as the weight for the corresponding observation equation. Finally, the normal equations for the parameter corrections are accumulated and solved by means of a standard weighted least squares process.

RESULTS

Three Modified L1 (ML1) lunar gravity models were derived from the orbital element data in Table 3, and are listed in Table 4. In the ML1.1 model, the C_{41} and S_{41} coefficients were determined from i and N data only, with the L1 model held fixed. For the ML1.2 model, the ML1.1 model was held fixed, and the C_{32} and S_{32} coefficients were derived from e and ω data. To derive the ML1.3 model, the L1 model again was held fixed, and the C_{32}, S_{32}, C_{41}, and S_{41} coefficients were solved for using the e, ω, i, and N data. The results substantiate the previously stated conclusion that the (3,2) coefficients would be basically determined from the e and ω data, and the (4,1) coefficients from the i and N data—the (3,2) values differ very little between the ML1.2 and ML1.3 models, and the same holds true for the (4,1) values in the ML1.1 and ML1.3 models.

Figures 1 through 32 show the fits to all the orbital element data for the L1, ML.1, ML1.2, and ML1.3 lunar gravity models. It is clear that the ML1 models fit all the inclination and node data as well as, or considerably better than, the L1 model does, with the single exception of the Apollo 8 inertial node. However, this node was much slower moving than the Apollo 10 and 11 nodes, so the fits are still quite comparable. In addition, the ML1.2 and ML1.3 models generally fit the e and ω data better than the models not containing the (3,2) coefficients, although the differences are not so pronounced. It should also be noted that the e and ω evolutions as predicted by the ML1.1 model are comparable to those predicted by the L1 model; at the same time, the ML1.1 model predicts the inclinations and inertial nodes much better than does the L1 model (with the previously noted minor exception). The "goodness of fits" are indicated in Table 5, which lists the root mean square of the observation residuals for each arc as produced by the L1, ML1.1, ML1.2, and ML1.3 lunar gravity models.

TESTS

In the initial stage of this work, the ROAD program was used to generate classical elements using the L1 lunar potential model. These were found to be in good agreement with those obtained from a different program (References 8, 9) for all Apollo and Lunar Orbiter cases that were considered. It was noted that the non-central portion of the lunar gravity field dominated the perturbations of not only the low altitude Apollo orbits but also many of the arcs of the more distant Lunar Orbiters with semimajor axes of a thousand kilometers larger. In addition, numerical integration of Apollo state vectors were made including not only the terms that dominate the motion but also the short period terms. The integrations were performed with all the third body effects included. These trajectories were in agreement with those published in Reference 8 and in this report.

The ML1.1 field was obtained first (Reference 10). Some preliminary tests of it were performed after which it was forwarded to the Manned Spacecraft Center (Reference 11). These tests have since been expanded to include the ML1.2 and ML1.3 fields, and to involve the processing of multi-revolution data arcs.

In order to determine the relative ability of the L1, the ML1.1, and the ML1.2 lunar gravity fields to model actual Apollo doppler tracking data, a series of tests were performed. Using the DEBTAP (Data Evaluation Branch Trajectory Analysis Program), a program which determines orbits of lunar satellites by means of weighted least squares, one revolution and two revolution arcs of doppler tracking data from Apollos 11 and 12 were processed. The list of standard-errors-of-fit presented in Table 6 is the result of this processing. Comparing standard-errors-of-fit, which are simply the square roots of the sums of the weighted residuals, is the simplest and most comprehensive method of comparing the goodness of fit of two orbit determinations. The results of the tests are quite clear cut. The L1 and the ML1.1 provide nearly identical data fitting capabilities. Based on the results presented in Table 6 it would be impossible to say which field was superior. The ML1.2 provides a somewhat degraded data fitting capability; the standard-errors-of-fit are perhaps 20% larger than for the L1 and ML1.1 in some cases. In other cases, some improvement was realized. The main conclusion to be drawn from this table is that the ML1.1 fits Apollo 11 and Apollo 12 tracking data as well as the L1 field.

In an attempt to show some significant superiority of one of the fields so far as fitting tracking data is concerned, an eight revolution, fifteen hour arc of two-way tracking data from Apollo 11 was processed. This data, from orbits 5 through 12, was processed with the Lungfish program. The standard deviations of fit for all four models appears in Table 7. Although the ML1.1 field better predicts the out-of-plane variables than does the L1 model, this fact does not seem to be reflected in these tracking data fits. The fact that the ML1.2 and ML1.3 fields better predict the in plane variables does manifest itself to some extent. Again, the main conclusion to be drawn here is that the ML1.1 field is as good as the L1 field so far as fitting tracking data is concerned.

The next test item was concerned with Lunar Orbiter trajectories. The L1, ML1.1, ML1.2, and ML1.3 models were used to generate classical elements at one day intervals for many Lunar Orbiter 2, 3, 4, and 5 arcs. As a result, several conclusions were drawn. First, the L1 and ML1.1

models produced nearly identical e, ω and N evolutions. Secondly, the ML1.1 was superior for inclination evolutions for the lowly inclined orbits when compared to the actual classical elements. For the highly inclined orbits, all four models performed equally as well. Thirdly, the ML1.2 and ML1.3 performed as well or better than the L1 and ML1.1 in all cases so far as e and ω evolutions are concerned. Examples to substantiate these conclusions can be found in Figures 33 to 35.

Finally, Table 8 contains a list of previous determinations of the (4,1) and (3,2) tesseral harmonics together with the values for these coefficients appearing in the various ML1 fields. The conclusion reached upon inspection of this table might be that the values of these coefficients obtained from Apollo orbits are in reasonable agreement with those obtained elsewhere, especially the (4,1) terms. This is fairly remarkable since the satellites used here were in very different type orbits, some of the other determinations were made directly from the tracking data, and the fields differ greatly in size.

DISCUSSION AND CONCLUSIONS

Very few efforts to obtain knowledge of the lunar gravity field have been made to date using data from Apollo missions. Only one of these efforts has been successful (Reference 3). The analysis performed in this report has been successful so far as predicting out of plane variables only. In addition, the rather good agreement between the various determinations of the (4,1) coefficients (Table 8) indicates that there is a substantial amount of gravity information implicitly contained in the classical elements of the Apollo orbits. The even zonal harmonics of a primary are best determined by the secular effects on its satellites. The remaining zonals and all the non-zonals must be determined from periodic perturbations of one kind or another. The only exceptions are cases of resonance. Therefore, it does not matter how long a satellite is in a particular orbit. The important question is concerned with how fast the angular variables that make up the arguments in the long period perturbations are moving.

In the case of the Apollo orbits, the arguments of perilune are moving very fast. Further, this is not simply due to the fact that Apollo orbits are nearly circular since the determinations of the orbits with the epoch at perilune reveals this rapid motion. Mathematically, then, this rapid motion in the argument of perilune provides us with many samples of the long period effects of the lunar potential on the classical element in a relatively short period of time.

Initially, we restricted ourselves to consider only gravity coefficients within a (4,4) field due to limitations of hardware, software, and in the interests of rapid computations. Only the terms of third degree were independent of multipliers of eccentricity in the perturbations in eccentricity and divisors of eccentricity in argument of perilune perturbations. However, it was our desire not to alter any of the coefficients in the already proven L1 model. This left only the (3,2) coefficient to consider so far as eccentricity and argument of perilune perturbations are concerned. The improvement with this single harmonic so far as eccentricity is concerned was for some cases disappointing; the fits to tracking data were inconsistent. However, this facet of the study was not without merit and the (3,2) coefficients may be of some practical application.

There seems to be little doubt, however, as to the merit of adopting the ML1.1 lunar gravity field as the operational model for Apollo orbit computations. We recommend the ML1.1 model. for several reasons:

1. The ML1.1 model vastly outperforms the L1 model for predicting out of plane variables for Apollo missions, while preserving the proven capabilities of the L1 field for in plane variables.
2. The ML1.1 model also predicts these out of plane elements for the posigrade Lunar Orbiters of moderate inclination as well or better than does the L1 model, even though the ML1.1 was derived from retrograde Apollo orbits.
3. The values for the (4,1) coefficients are consistent with values obtained from Lunar Orbiter analyses.
4. The fits to Apollo tracking data for one, two, and eight revolution arcs are as good for ML1.1 as they are for L1.

The non-zonal harmonics in the L1 field are all symmetric with respect to the reference longitude (that is, $S_{22} = S_{31} = S_{33} = 0$). The (4,1) harmonic in the ML1.1 field is not. In fact, there is an accomodation between the proposed values for the (4,1) harmonic and the local gravity effects first observed on Lunar Orbiters (Reference16), and which were called "mascons." In Figure 36, the shaded areas represent positive gravity anomalies due to the (4,1) harmonic. It is clear that this subdivision is in accord with many of the mascon efforts. This, in itself, does not justify adopting this harmonic. The justifications appeared above. It would, however, move the operational Apollo lunar gravity field one quantum jump closer to accomodation with the mascon results.

REFERENCES

1. Jeffreys, H., *Monthly Notices of the Royal Astronomical Society,* 122(5), pp. 431-432, 1961.

2. Risdal, R. E., "Development of a Simple Lunar Model for Apollo", Contract Report D2-100819-1, The Boeing Co., Seattle, Wash., 1968.

3. Compton, H. R., and Tolson, R. H., "Study of a Simple Lunar Gravitational Model for Application to Apollo Orbit Determination and Prediction", Langley Research Center, June 11, 1969 (memo to J. C. McPherson, Manned Spacecraft Center, Houston).

4. "Lunar Model Analysis for Apollo 12", TRW Systems Group, Redondo Beach, Calif., Aug. 31, 1969.

5. "Apollo 12 MSFN Metric Tracking Performance", GSFC X-832-70-79, March 1970.

6. Hagihara, Y., *Astronomical Journal*, Vol. 67, p. 108, 1962.

7. "ROAD—Program Description and User's Guide", Wolf Research and Development Corp., Riverdale, Md. (prepared for NASA-GSFC under contract No. NAS-5-9756-182), 1970.

8. Diamant, L. S., "Explanatory Supplement to the Mean-Element Lunar Potential Model Catalogs", TRW Letter 5522.7-70-49, 26 March 1970.

9. Diamant, L. S., "Mean-Element Lunar Potential Model Catalog, Model L-1," TRW Letter 5522.7-70-76, 7 May 1970.

10. Murphy, J. P., "A Modified L1 Field for Accurate Inclination and Inertial Node Predictions for Apollo Orbits", June 11, 1970 (memo to J. Barsky, Manned Flight Planning and Analysis Division).

11. Barsky, J., "An Augmented L1 Lunar Potential Model Suggested by J. Murphy of Mission Trajectory Determination Branch of Goddard Space Flight Center", June 23, 1970 (memo to J. McPherson, Mathematical Physics Branch, Mission Planning and Analysis Division, Manned Spacecraft Center).

12. Lorell, J., "Lunar Orbiter Gravity Analysis", Technical Report 32-1387, Jet Propulsion Laboratory, Pasadena, Calif., June 15, 1969.

13. Tolson, R. H., and Gapcynski, J. P., "An Analysis of the Lunar Gravitational Field as Obtained from Lunar Orbiter Tracking Data", presented at the IQSY/COSPAR Assemblies, London, England, July 17-28, 1967.

14. Gapcynski, J. P., Blackshear, W. T., and Compton, H. R., "The Lunar Gravitational Field as Determined from the Tracking Data of the Lunar Orbiter Series of Spacecraft", presented at the AIAA-AAS Astrodynamics Specialists Conference, Grand Teton National Park, Wyoming, September 3-5, 1968.

15. Blackshear, W. T., "Progress on Lunar Gravitational Potential Determinations by Analysis of Lunar Orbiter Tracking Data" presented at the AGU 50th Annual Meeting, Washington, D. C., April 1969.

16. Muller, P. M. and Sjogren, W. L., *Science,* Vol. 161, page 680 (1968).

Table 1

Apollo Operational Lunar Gravity Models.*

COEFFICIENT	TRI-AXIAL	R2	L1
C_{20}	-2.0718677	-2.07108	-2.07108
C_{22}	0.20239141	0.20716	0.20715
C_{30}		0.21	0.21
C_{31}		0.34	0.34
C_{33}			0.02583

* Multiply all coefficients by 10^{-4}

NASA-GSFC-T&DS
MISSION & TRAJECTORY ANALYSIS DIVISION
BRANCH 552 DATE July 1970
BY J. P. Murphy PLOT NO. 2169

Table 2

Apollo Classical Element Data Arcs.

ARC	MISSION	ORBIT NUMBERS	"FREE FLIGHT" PERIOD
1	APOLLO 8	3, 4, 5, 6, 7, 8, 9, 10	CIRCULARIZATION TO TEI
2	APOLLO 10	3, 4, 5, 6, 7, 8, 9, 10, 11, 13, 14, 15	CIRCULARIZATION TO EVASIVE MANEUVER
3	APOLLO 10	17, 18, 19, 20, 21, 22, 24, 25, 26, 27, 28, 29, 30, 31	EVASIVE MANEUVER TO TEI
4	APOLLO 11	3, 4, 5, 6, 7, 8, 9, 10, 11, 12, 13	CIRCULARIZATION TO CSM/LM SEPARATION
5	APOLLO 11	14, 15, 16, 17, 18, 19, 20, 21, 22, 23, 24, 26, 27	CSM/LM SEPARATION TO TEI
6	APOLLO 12	3, 4, 5, 6, 7, 8, 9, 10, 11, 12	CIRCULARIZATION TO CSM/LM SEPARATION
7	APOLLO 12	20, 21, 22, 23, 24, 25, 26, 27, 28, 29, 30, 32	PLANE CHANGE TO CSM/LM DOCKING
8	APOLLO 12	39, 40, 41, 42, 43, 44, 45	PLANE CHANGE TO TEI

NASA-GSFC-T&DS
MISSION & TRAJECTORY ANALYSIS DIVISION
BRANCH 552 DATE July 1970
BY J. P. Murphy PLOT NO. 2170

Table 3

Apollo Classical Element Histories.

ARC 1 APOLLO 8

TIME(MJD)	a(M.R.)	e	i(DEG.)	ω(DEG.)	N(DEG.)	M(DEG.)
40214.6117331	1.06434684	.0007980	167.6871	295.4667	50.3879	0.0
40214.6976670	1.06433545	.0010360	167.7067	310.2070	50.5119	0.0
40214.7812877	1.06428564	.0013120	167.7108	314.8446	50.6251	0.0
40214.8644853	1.06425793	.0015970	167.7201	317.6396	50.7262	0.0
40214.9474647	1.06422146	.0018930	167.7190	319.4810	50.8095	0.0
40215.0302992	1.06419200	.0021700	167.7444	320.8273	51.0147	0.0
40215.1128475	1.06412448	.0024310	167.7534	320.8720	51.1573	0.0
40215.1957676	1.06414903	.0027220	167.7465	322.4264	51.1694	0.0

ARC 2 APOLLO 10

TIME(MJD)	a(M.R.)	e	i(DEG.)	ω(DEG.)	N(DEG.)	M(DEG.)
40363.0428336	1.06291814	.0008390	178.7469	35.0556	181.8886	0.0
40363.1360199	1.06291762	.0008660	178.8032	40.1027	184.2050	0.0
40363.2208300	1.06284642	.0010630	178.8184	50.7362	184.2495	0.0
40363.3052676	1.06274243	.0012300	178.8412	60.3651	184.9274	0.0
40363.3886009	1.06271069	.0014860	178.8890	63.9567	185.9713	0.0
40363.4710500	1.06271349	.0017470	178.8797	66.9879	187.1131	0.0
40363.5537603	1.06270823	.0020060	178.9009	69.4209	188.1167	0.0
40363.6361845	1.06264492	.0022540	178.9096	70.9939	189.5160	0.0
40363.7194735	1.06256917	.0024470	178.9422	74.5174	189.0592	0.0
40363.8837527	1.06242940	.0028970	178.9535	76.1084	192.4977	0.0
40363.9660240	1.06243238	.0031960	179.0009	76.4989	193.2508	0.0
40364.0481611	1.06238328	.0034650	178.9478	76.6095	194.3073	0.0

ARC 3 APOLLO 10

TIME(MJD)	a(M.R.)	e	i(DEG.)	ω(DEG.)	N(DEG.)	M(DEG.)
40364.2150285	1.06317523	.0043080	178.9779	88.0071	180.9614	0.0
40364.2976785	1.06340969	.0044660	179.0050	89.1406	181.2861	0.0
40364.3799058	1.06342670	.0047460	179.0232	89.5754	182.7999	0.0
40364.4621410	1.06343144	.0050290	179.0559	89.8224	184.0953	0.0
40364.5443889	1.06343074	.0053150	179.0518	90.0000	185.2606	0.0
40364.6266194	1.06339514	.0055760	179.0651	90.4865	186.8180	0.0
40364.7911922	1.06343758	.0062280	179.1188	91.5016	189.4640	0.0
40364.8735225	1.06344354	.0065080	179.1128	91.1077	189.7110	0.0
40364.9558955	1.06347458	.0067870	179.1127	91.9069	190.9754	0.0
40365.0382494	1.06347896	.0070620	179.0947	92.6186	192.2488	0.0
40365.1205243	1.06345441	.0073550	179.1445	93.0802	193.6127	0.0
40365.2028104	1.06345108	.0076430	179.1557	93.1635	194.5558	0.0
40365.2851356	1.06347212	.0079370	179.1725	92.9556	195.0129	0.0
40365.3674532	1.06345599	.0082500	179.1904	92.8459	195.6209	0.0

ARC 4 APOLLO 11

TIME(MJD)	a(M.R.)	e	i(DEG.)	ω(DEG.)	N(DEG.)	M(DEG.)
40421.9629387	1.06242502	.0059770	178.4394	249.5599	167.5323	0.0
40422.0454810	1.06247342	.0057050	178.4649	250.5962	167.8274	0.0
40422.1281541	1.06241011	.0054790	178.4550	255.5073	171.4219	0.0
40422.2109644	1.06236627	.0052290	178.4656	259.5616	173.5490	0.0
40422.2936987	1.06238784	.0049900	178.4800	256.7675	172.1653	0.0
40422.3770300	1.06242940	.0047630	178.4647	260.4040	171.1459	0.0
40422.4592083	1.06248219	.0045380	178.4915	259.8027	168.8719	0.0
40422.5420609	1.06251866	.0043210	178.5217	264.7934	171.7437	0.0
40422.6248772	1.06236153	.0041610	178.5222	267.9222	172.8766	0.0
40422.7062675	1.06255040	.0040040	178.5871	265.4301	174.7143	0.0
40422.7900919	1.06238118	.0037890	178.5766	271.4727	174.3289	0.0

NASA-GSFC-T&DS
MISSION & TRAJECTORY ANALYSIS DIVISION
BRANCH 552 DATE July 1970
BY J P. Murphy PLOT NO. 2171

Table 3 (Continued)

ARC 5 APOLLO 11

TIME(MJD)	a(M.R.)	e	i(DEG.)	ω(DEG.)	N(DEG.)	M(DEG.)
40422.8718940	1.06231331	.0039640	178.5915	269.9769	163.2371	0.0
40422.9548903	1.06236750	.0037580	178.5875	271.7263	162.1272	0.0
40423.0379747	1.06234978	.0035680	178.5897	276.4500	163.5866	0.0
40423.1216486	1.06226403	.0034620	178.6448	284.7647	166.0358	0.0
40423.2046242	1.06232822	.0033250	178.6532	288.3690	165.3336	0.0
40423.2885118	1.06236978	.0032300	178.6658	294.3839	166.0860	0.0
40423.3771338	1.06242221	.0031600	178.6897	300.5971	166.6814	0.0
40423.4558624	1.06247009	.0031220	178.7099	307.1191	167.1189	0.0
40423.5397081	1.06250165	.0031280	178.7491	314.3773	167.7763	0.0
40423.6235247	1.06256075	.0031330	178.7525	321.5304	168.4644	0.0
40423.7073586	1.06260161	.0031810	178.7654	328.5203	168.9111	0.0
40423.8748308	1.06262335	.0033830	178.7984	341.9411	170.0995	0.0
40423.9567812	1.06229490	.0035870	178.8136	341.8256	171.5603	0.0

ARC 6 APOLLO 12

TIME(MJD)	a(M.R.)	e	i(DEG.)	ω(DEG.)	N(DEG.)	M(DEG.)
40543.3961227	1.06277983	.0059077	164.8270	68.1980	337.1260	359.0230
40543.4786806	1.06278098	.0056158	164.7680	67.2900	337.2826	0.6490
40543.5607639	1.06277696	.0053223	164.7840	65.9770	337.3070	0.4450
40543.6427454	1.06279939	.0050288	164.7360	64.6160	337.4881	0.0020
40543.7249537	1.06276890	.0047463	164.7460	63.6210	337.4952	0.0170
40543.8071759	1.06277523	.0044672	164.7410	62.0570	337.5724	0.7290
40543.8888889	1.06274244	.0041852	164.7350	60.6490	337.6050	359.0060
40543.9711921	1.06278041	.0039208	164.7060	58.6020	337.7523	0.6310
40544.0536720	1.06278156	.0036729	164.6840	56.6510	337.8539	2.8950
40544.1348432	1.06276142	.0034020	164.6060	53.9370	338.1004	0.3180

ARC 7 APOLLO 12

TIME(MJD)	a(M.R.)	e	i(DEG.)	ω(DEG.)	N(DEG.)	M(DEG.)
40544.7888079	1.06363710	.0020915	165.6460	41.5060	334.5390	2.5370
40544.8701736	1.06303068	.0018479	165.6040	36.3560	334.6430	2.9850
40544.9501273	1.06307211	.0016722	165.5900	28.6730	334.7336	359.7710
40545.0305852	1.06295013	.0014525	165.5630	21.7210	334.8238	359.8040
40545.1103935	1.06318890	.0014838	165.5430	7.9635	334.9517	0.3160
40545.1900926	1.06325104	.0014798	165.5400	355.4483	334.9864	0.7780
40545.2695718	1.06332583	.0015524	165.4870	341.9360	335.1815	1.4350
40545.3486690	1.06336956	.0016750	165.5230	328.4270	335.1336	0.1640
40545.4278935	1.06333734	.0017711	165.5110	317.0230	335.1912	2.5440
40545.5094444	1.06331433	.0018950	165.4960	309.0470	335.2486	1.4920
40545.5899306	1.06340868	.0021964	165.4130	303.1750	335.7792	359.2350
40545.7509028	1.06318085	.0024588	165.3940	285.2880	335.6828	359.6990

ARC 8 APOLLO 12

TIME(MJD)	a(M.R.)	e	i(DEG.)	ω(DEG.)	N(DEG.)	M(DEG.)
40546.3253009	1.06345931	.0039980	168.7580	282.6870	326.4160	0.1480
40546.4072454	1.06332411	.0041290	168.6980	278.5620	326.2636	1.7830
40546.4887188	1.06329074	.0043590	168.6480	276.1120	326.4581	357.6920
40546.5701389	1.06329994	.0046261	168.6420	274.0240	326.4808	357.4490
40546.6527546	1.06332986	.0048950	168.6360	272.1260	326.5662	0.0450
40546.7347222	1.06329362	.0051364	168.6050	270.4590	326.7211	359.5780
40546.8171759	1.06335518	.0054255	168.5820	269.3420	327.0103	0.8630

NASA-GSFC-T&DS
MISSION & TRAJECTORY ANALYSIS DIVISION
BRANCH 552 DATE July 1970
BY J. P. Murphy PLOT NO. 2171

Table 4

Modified L1 (ML1) Lunar Gravity Models.*

COEFFICIENT	ML1.1	ML1.2	ML1.3
C_{20}	-2.07108	-2.07108	-2.07108
C_{22}	0.20715	0.20715	0.20715
C_{30}	0.21	0.21	0.21
C_{31}	0.34	0.34	0.34
C_{32}		0.1012	0.1040
S_{32}		0.06790	0.07282
C_{33}	0.02583	0.02583	0.02583
C_{41}	-0.1284	-0.1284	-0.1083
S_{41}	0.1590	0.1590	0.1460

*Multiply all coefficients by 10^{-4}

NASA-GSFC-T&DS
MISSION & TRAJECTORY ANALYSIS DIVISION
BRANCH 552 DATE July 1970
BY J. P. Murphy PLOT NO. 2172

Table 5

Root Mean Squares of Observation Residuals.

CLASSICAL ELEMENTS	ARC NO.	ROOT MEAN SQUARE			
		L1	ML1.1	ML 1.2	ML 1.3
e	1	.0000894	.0000900	.000115	.000118
	2	.000265	.000298	.000545	.000499
	3	.000116	.000124	.000129	.000132
	4	.000257	.000253	.000145	.000143
	5	.00101	.00101	.000761	.000779
	6	.000401	.000399	.000107	.000123
	7	.000443	.000546	.000161	.000153
	8	.000136	.000163	.0000985	.000102
i (degrees)	1	.0266	.00826	.00825	.00822
	2	.112	.0286	.0285	.0371
	3	.119	.0154	.0153	.0242
	4	.0799	.0222	.0220	.0222
	5	.135	.0120	.0120	.0236
	6	.0946	.0256	.0255	.0268
	7	.117	.0235	.0235	.0258
	8	.0844	.0205	.0203	.0259
ω (degrees)	1	10.4	10.4	2.48	2.60
	2	5.49	8.43	2.99	2.62
	3	1.60	5.70	3.86	2.97
	4	13.0	10.4	3.65	3.76
	5	14.5	11.3	4.69	4.71
	6	4.62	5.56	.406	.386
	7	21.8	22.1	1.79	1.74
	8	4.52	4.17	1.30	1.22
Ω (degrees)	1	.0911	.224	.224	.199
	2	6.49	.489	.486	1.02
	3	9.01	.575	.597	1.20
	4	4.35	1.73	1.73	1.77
	5	3.88	.660	.660	.858
	6	.100	.101	.101	.0968
	7	.149	.155	.155	.151
	8	.128	.125	.125	.124

NASA-GSFC-T&DS
MISSION & TRAJECTORY ANALYSIS DIVISION
BRANCH 552 DATE July 1970
BY J P. Murphy PLOT NO. 2173

Table 6

Standard Errors of Fit to Apollo 11 and Apollo 12 Range and Range-Rate Tracking Data.

APOLLO MISSION	ORBIT NUMBER(S)	STANDARD ERROR OF FIT (dimensionless)		
		L1	ML1.1	ML1.2
11	8	2.89	2.89	3.00
11	9	2.65	2.67	2.77
11	18	2.31	2.31	2.38
11	19	3.00	3.01	3.12
11	29	2.93	2.99	3.03
11	8 and 9	19.2	19.0	17.7
11	18 and 19	15.9	15.1	14.3
12	9	18.4	18.1	23.4
12	10	17.8	17.9	24.6
12	16	18.8	18.8	24.5
12	17	21.4	20.7	26.0
12	40	15.4	15.2	18.6
12	41	14.5	14.3	17.2
12	42	15.9	15.8	20.3
12	9 and 10	33.2	28.2	28.0
12	40 and 41	31.6	32.1	

NASA-GSFC-T&DS
MISSION & TRAJECTORY ANALYSIS DIVISION
BRANCH 552 DATE July 1970
BY J. P. Murphy PLOT NO. 2174

Table 7

Standard Deviations of Fit to a Fifteen Hour Arc of Apollo 11 Two-Way Doppler Observations.

LUNAR GRAVITY MODEL	STANDARD DEVIATION (CPS)
L1	4.133
ML1.1	4.109
ML1.2	3.771
ML1.3	3.758

NASA-GSFC-T&DS
MISSION & TRAJECTORY ANALYSIS DIVISION
BRANCH 552 DATE July 1970
BY J. P Murphy PLOT NO. 2175

Table 8

Values for (4,1) and (3,2) Coefficients.*

SOURCE	REFERENCE	$C_{4,1}$	$S_{4,1}$	$C_{3,2}$	$S_{3,2}$
ML1.1	10	-.1284	.1590		
ML1.2	THIS REPORT	-.1284	.1590	.1012	.0679
ML1.3	THIS REPORT	-.1083	.1460	.1040	.0728
JPL-1	12	-.1237	.0564	-.0257	-.0200
JPL-2	12	-.1063	.0755	.0003	.0277
JPL-3	12	-.1607	.1099	.0076	.0283
LaRC (5x5)	13	-.1560	.0391	.1294	-.0147
LaRC (7x7)	14	.0813	-.0172	.0693	.0441
LaRC (13x13)	15	-.0573	.0680	.0502	.0203

*Multiply all coefficients by 10^{-4}.

NASA-GSFC-T&DS
MISSION & TRAJECTORY ANALYSIS DIVISION
BRANCH 552 DATE July 1970
BY J. P. Murphy PLOT NO. 2176

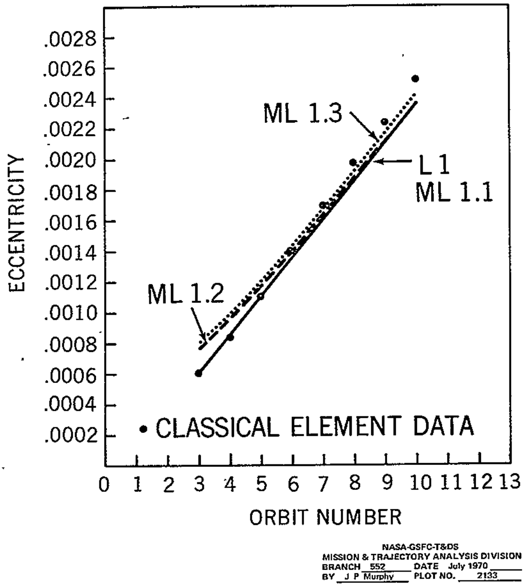

Figure 1—Arc 1 - Apollo 8 eccentricity vs orbit number.

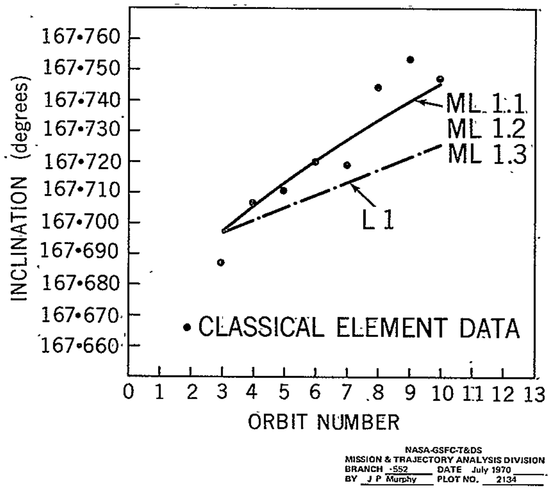

Figure 2—Arc 1 - Apollo 8 inclination vs orbit number.

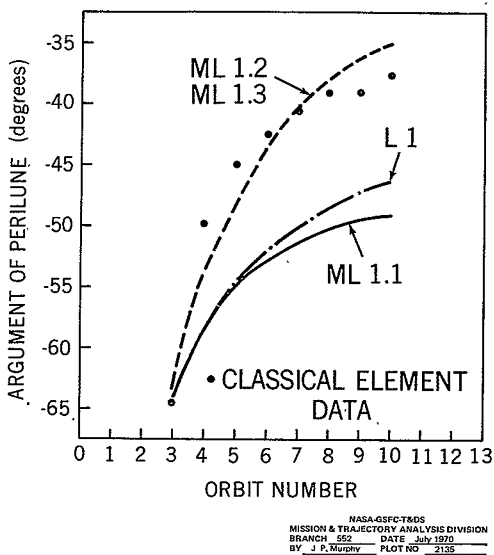

Figure 3—Arc 1 - Apollo 8 argument of perilune vs orbit number.

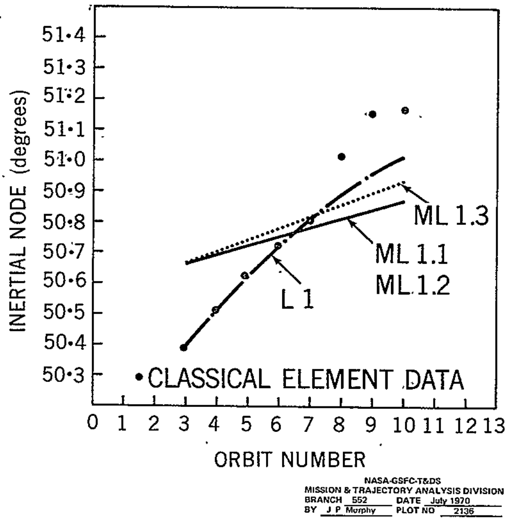

Figure 4—Arc 1 - Apollo 8 inertial node vs orbit number.

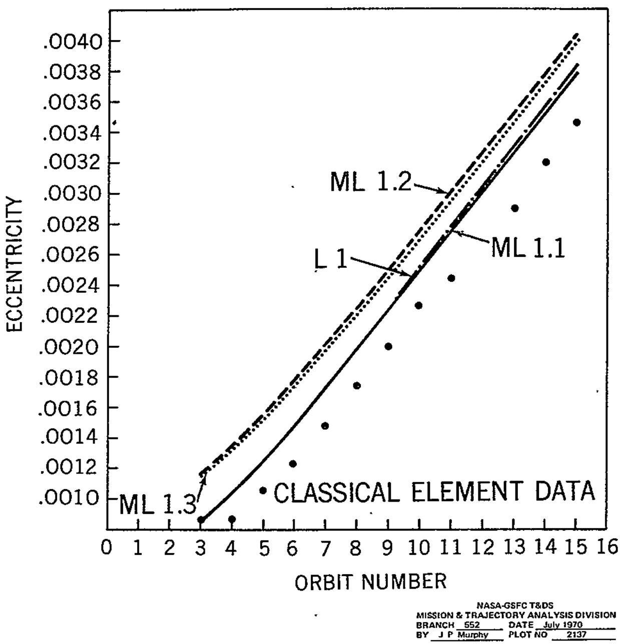

Figure 5—Arc 2 - Apollo 10 eccentricity vs orbit number.

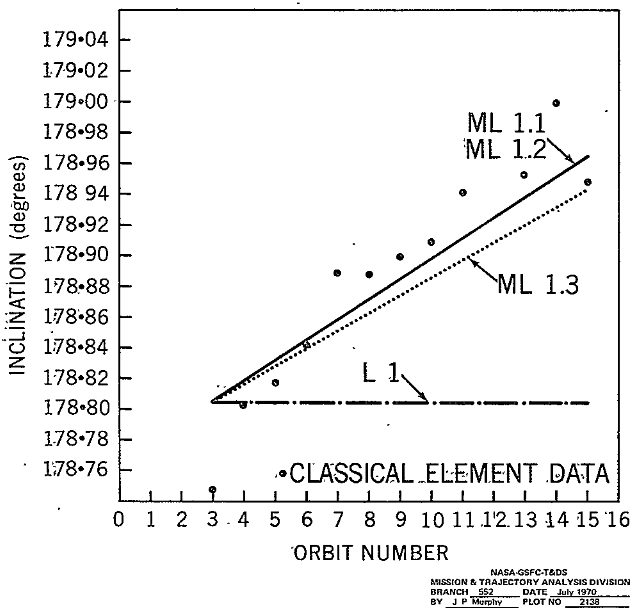

Figure 6—Arc 2 - Apollo 10 inclination vs orbit number.

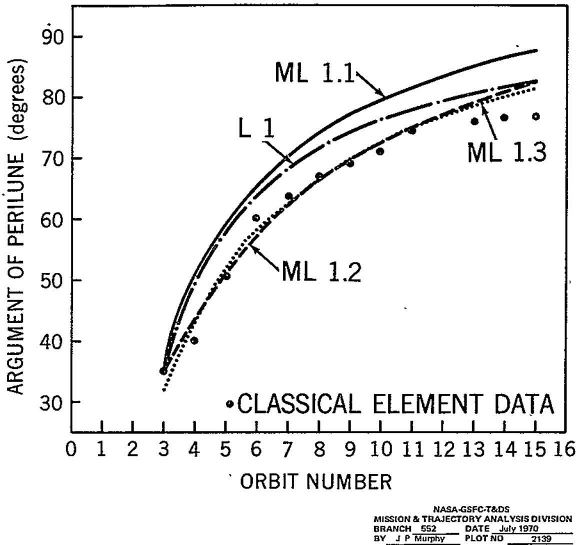

Figure 7—Arc 2 - Apollo 10 argument of perilune vs orbit number.

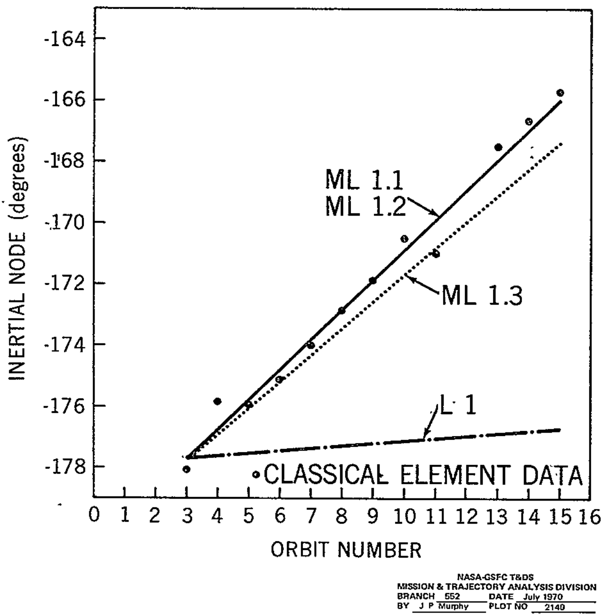

Figure 8—Arc 2 - Apollo 10 inertial node vs orbit number.

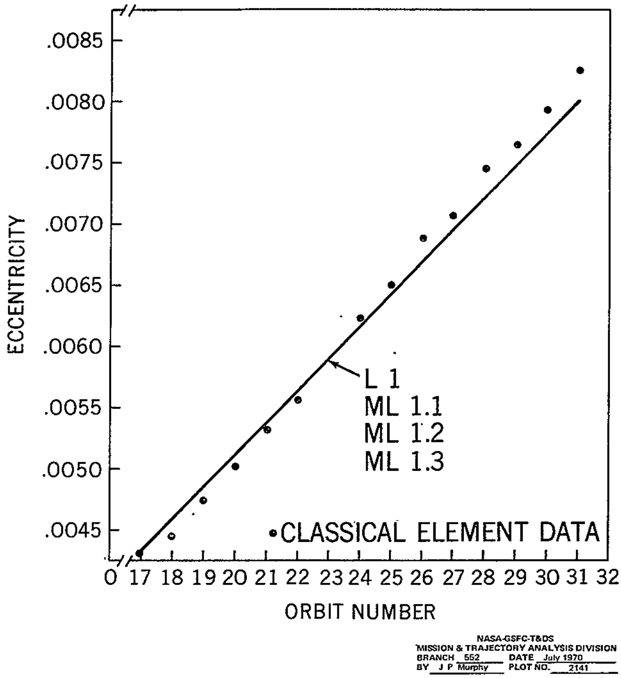

Figure 9—Arc 3 – Apollo 10 eccentricity vs orbit number.

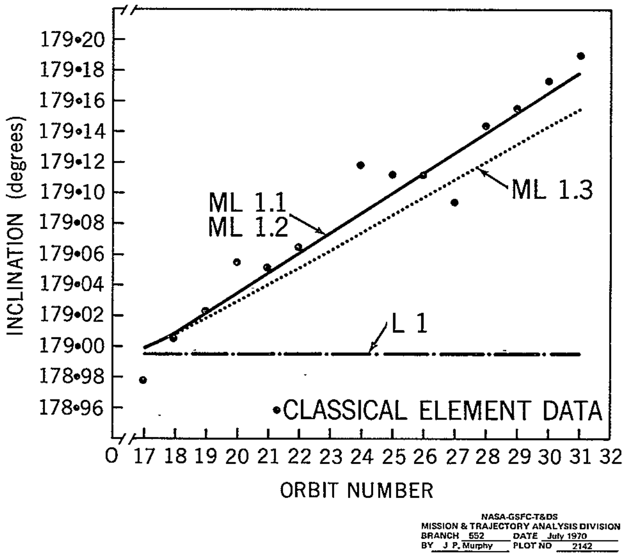

Figure 10—Arc 3 - Apollo 10 inclination vs orbit number.

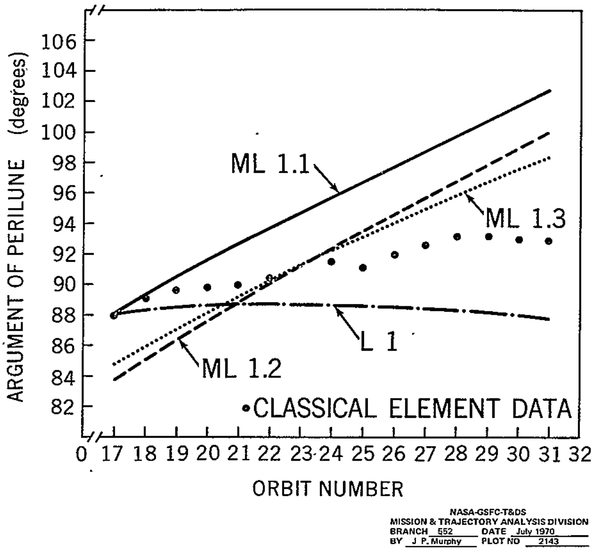

Figure 11—Arc 3 - Apollo 10 argument of perilune vs orbit number.

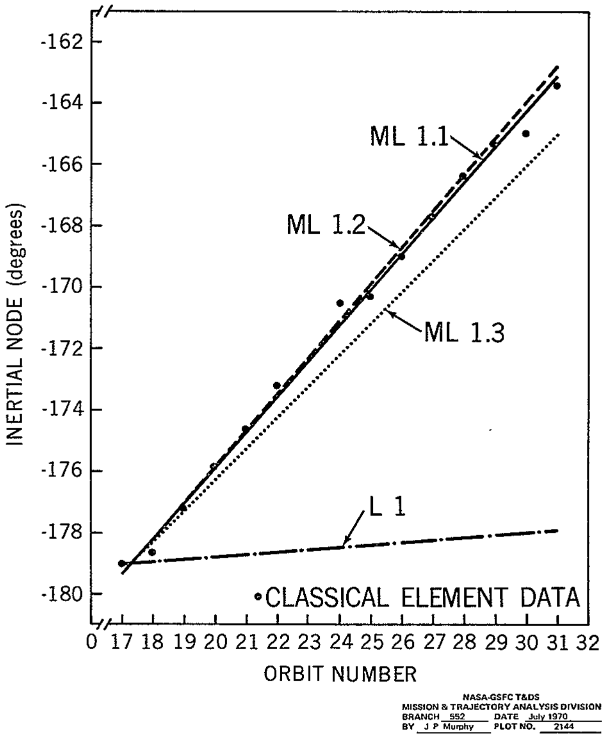

Figure 12—Arc 3 - Apollo 10 inertial node vs orbit number.

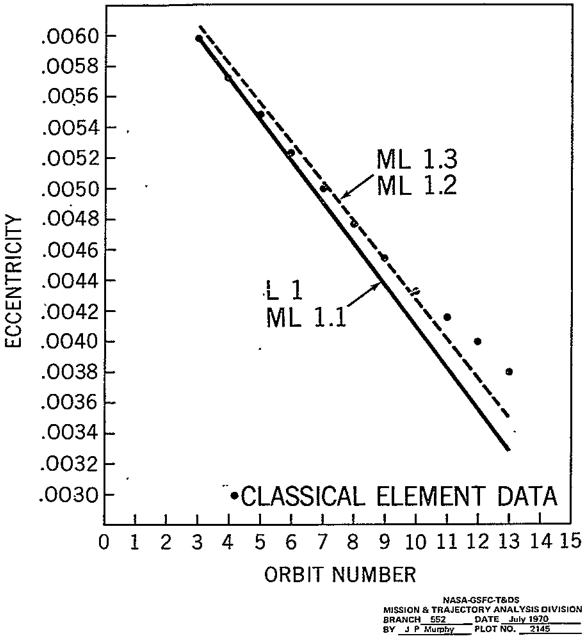

Figure 13—Arc 4 - Apollo 11 eccentricity vs orbit number.

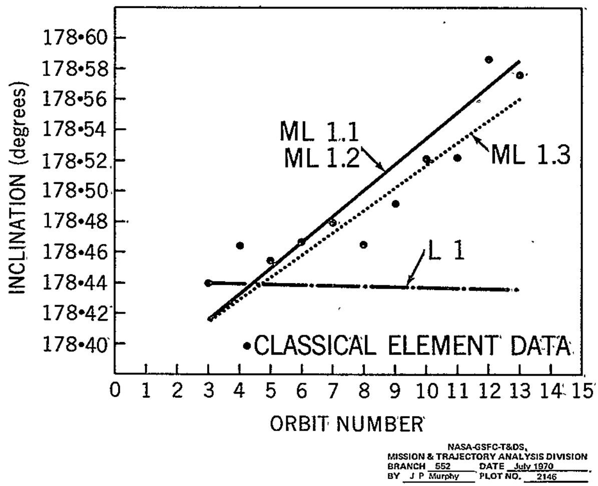

Figure 14—Arc 4 – Apollo 11 inclination vs orbit number.

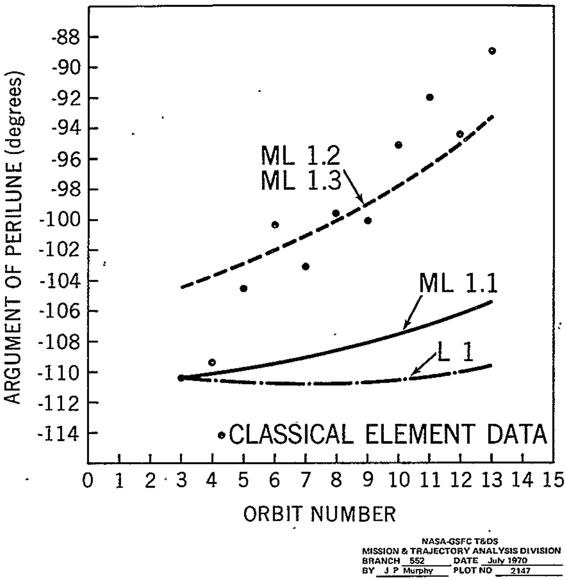

Figure 15—Arc 4 - Apollo 11 argument of perilune vs orbit number.

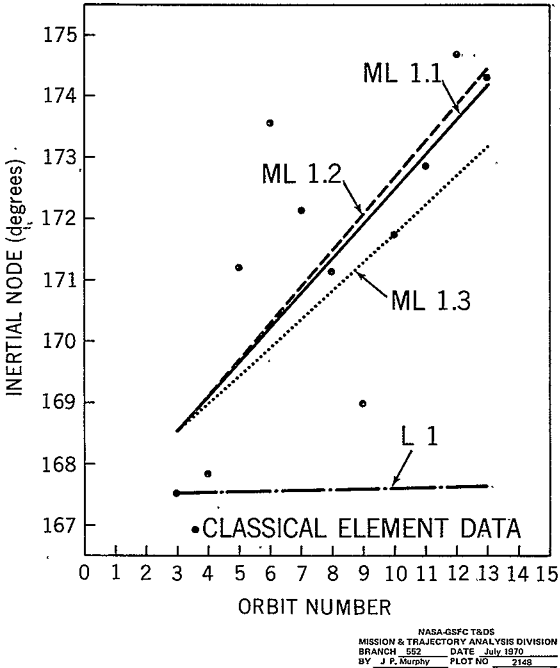

Figure 16—Arc 4 - Apollo 11 inertial node vs orbit number.

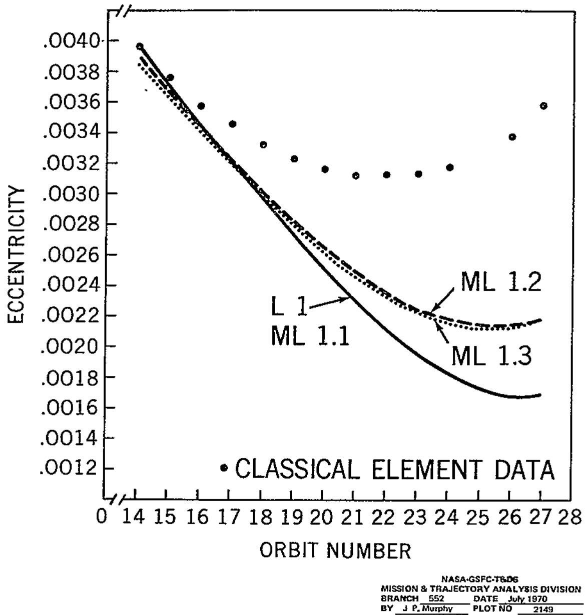

Figure 17—Arc 5 - Apollo 11 eccentricity vs orbit number.

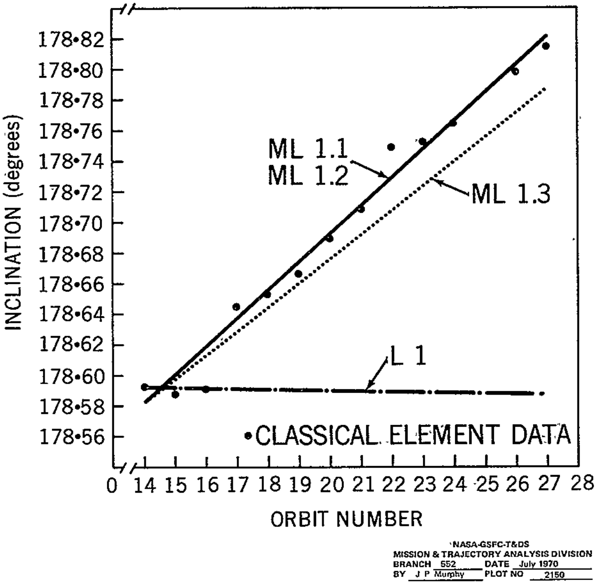

Figure 18—Arc 5 - Apollo 11 inclination vs orbit number.

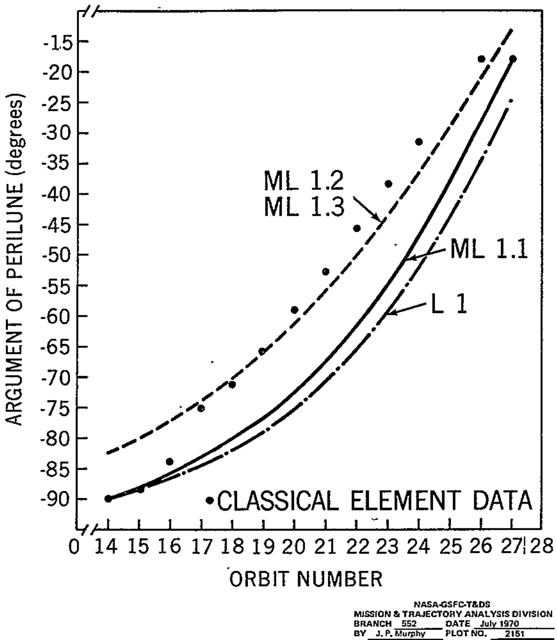

Figure 19—Arc 5 - Apollo 11 argument of perilune vs orbit number.

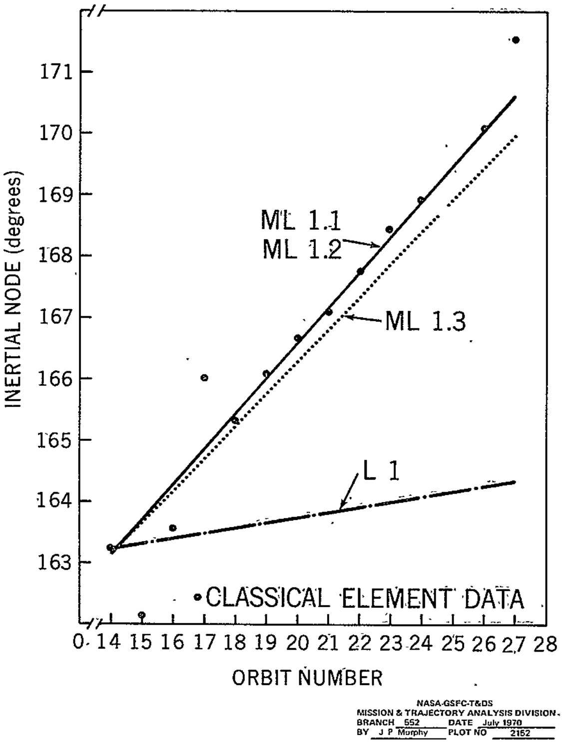

Figure 20—Arc 5 - Apollo 11 inertial node vs orbit number.

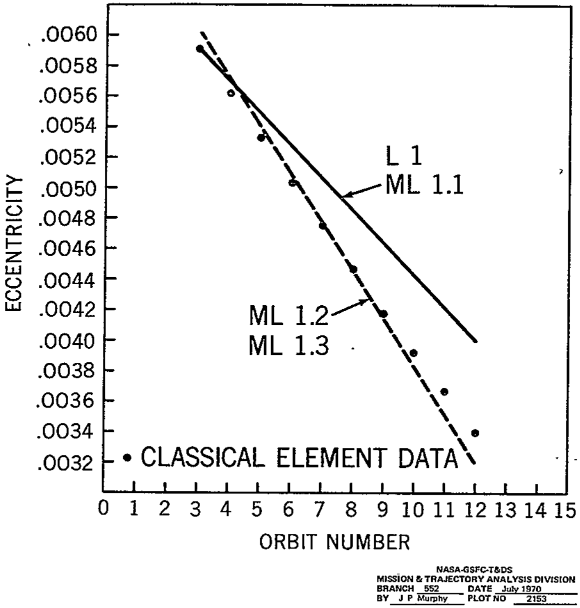

Figure 21—Arc 6 - Apollo 12 eccentricity vs orbit number.

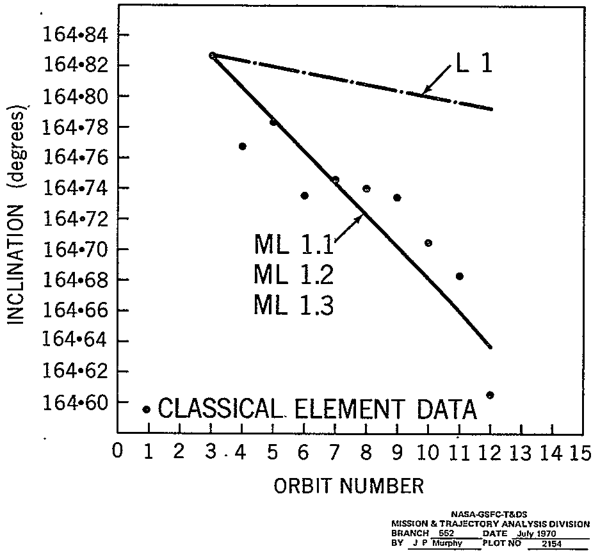

Figure 22—Arc 6 - Apollo 12 inclination vs orbit number.

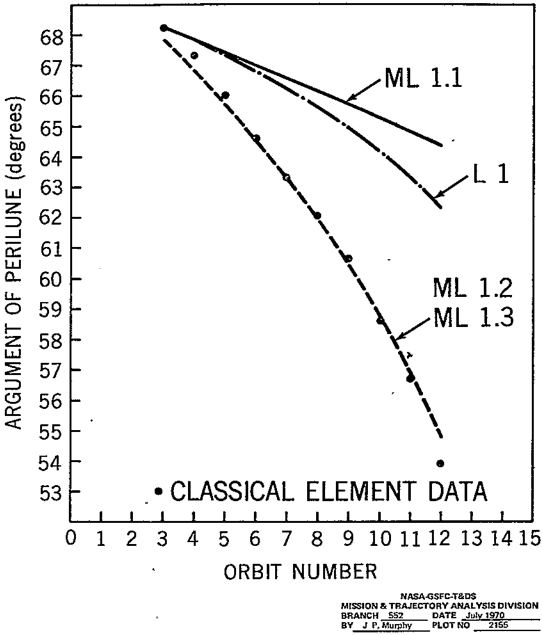

Figure 23—Arc 6 – Apollo 12 argument of perilune vs orbit number.

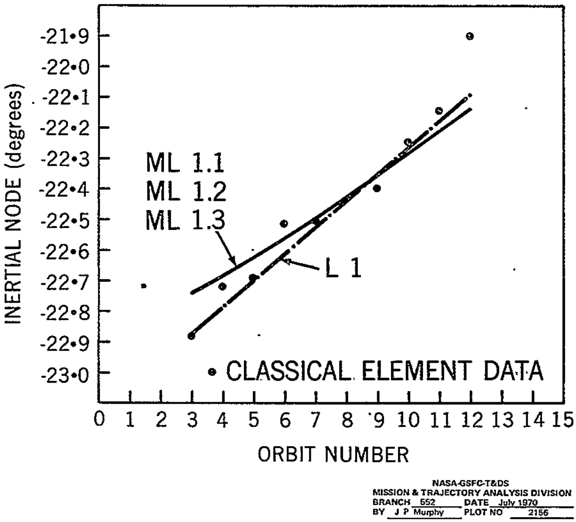

Figure 24—Arc 6 – Apollo 12 inertial node vs orbit number.

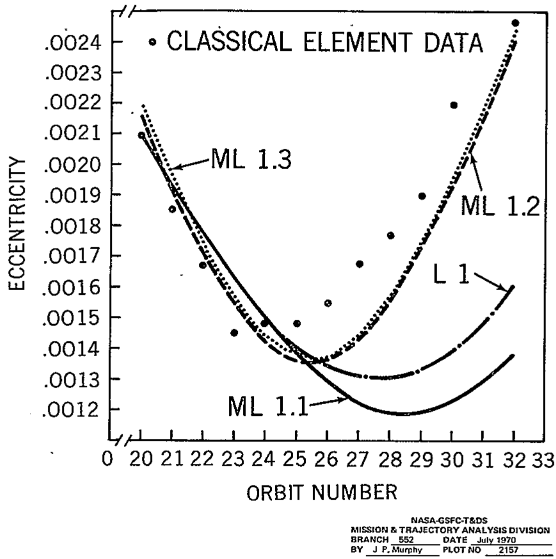

Figure 25—Arc 7 - Apollo 12 eccentricity vs orbit number.

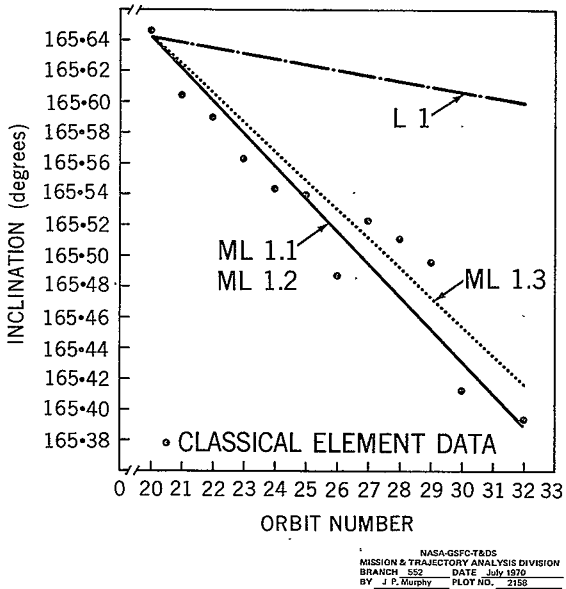

Figure 26—Arc 7 - Apollo 12 inclination vs orbit number.

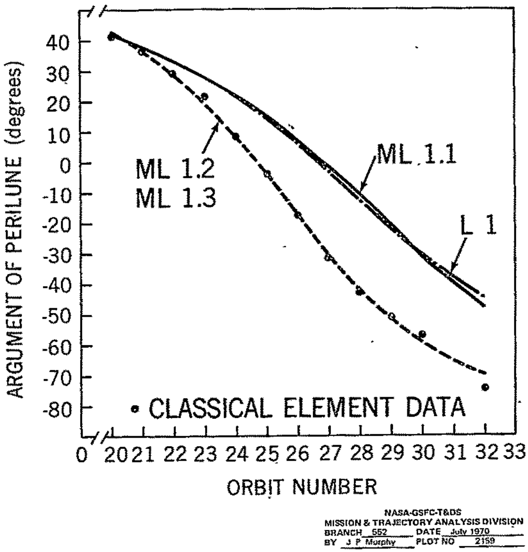

Figure 27—Arc 7 - Apollo 12 argument of perilune vs orbit number.

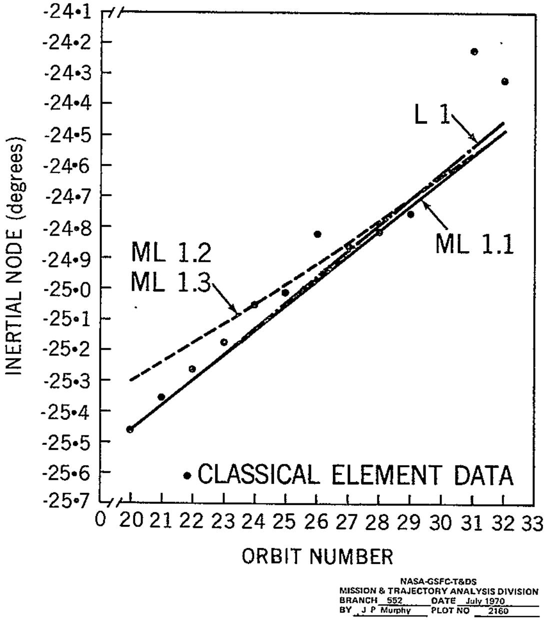

Figure 28—Arc 7 - Apollo 12 inertial node vs orbit number.

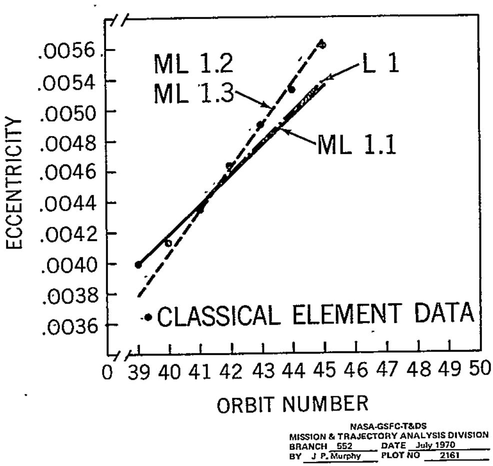

Figure 29—Arc 8 - Apollo 12 eccentricity vs orbit number.

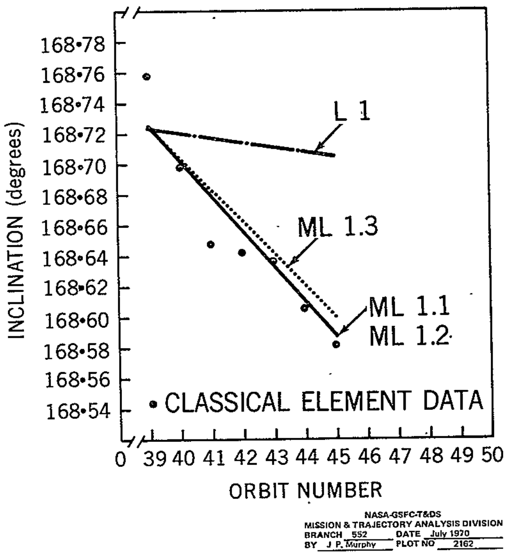

Figure 30—Arc 8 - Apollo 12 inclination vs orbit number.

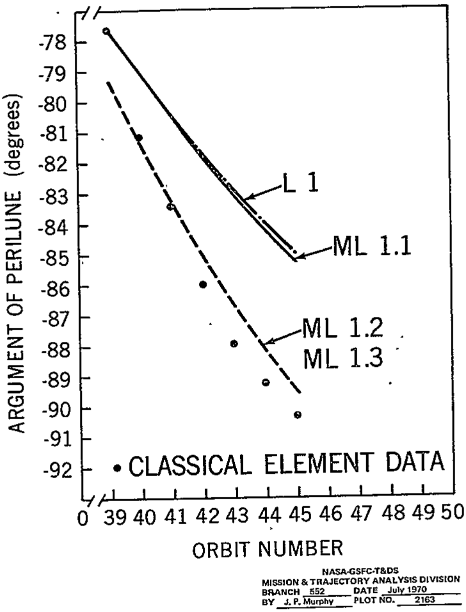

Figure 31—Arc 8 - Apollo 12 argument of perilune vs orbit number.

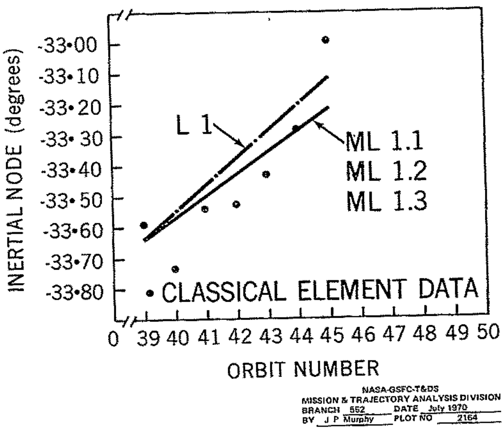

Figure 32—Arc 8 - Apollo 12 inertial node vs orbit number.

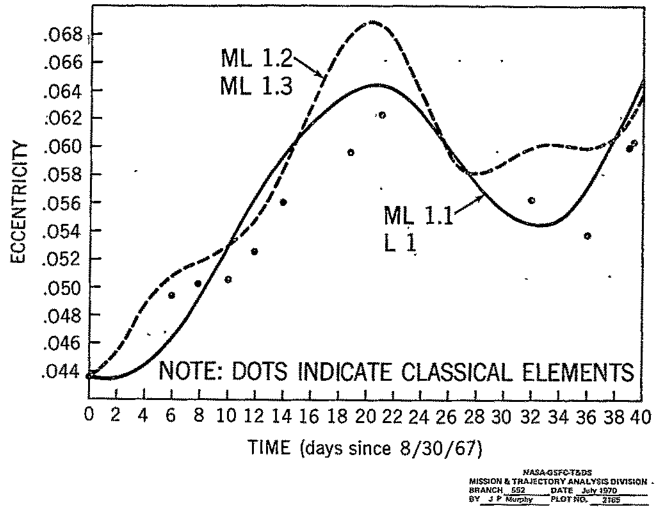

Figure 33—Lunar Orbiter 3 eccentricity vs time.

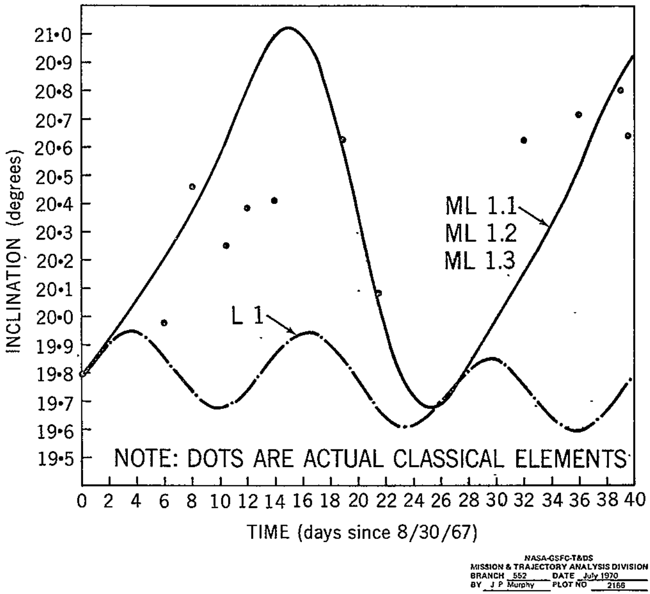

Figure 34—Lunar Orbiter 3 inclination vs time.

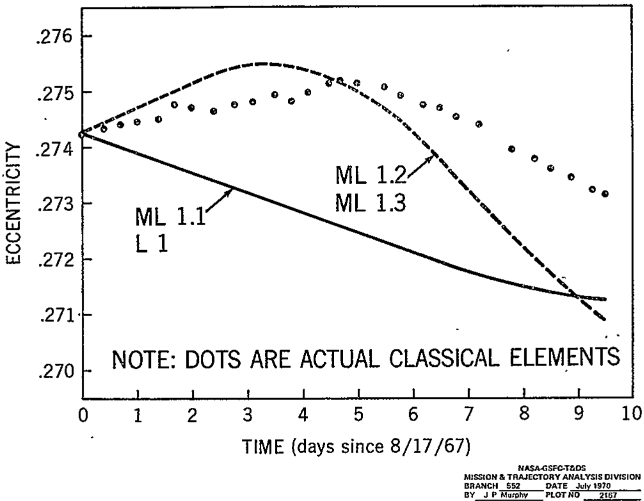

Figure 35—Lunar Orbiter 5 eccentricity vs time.

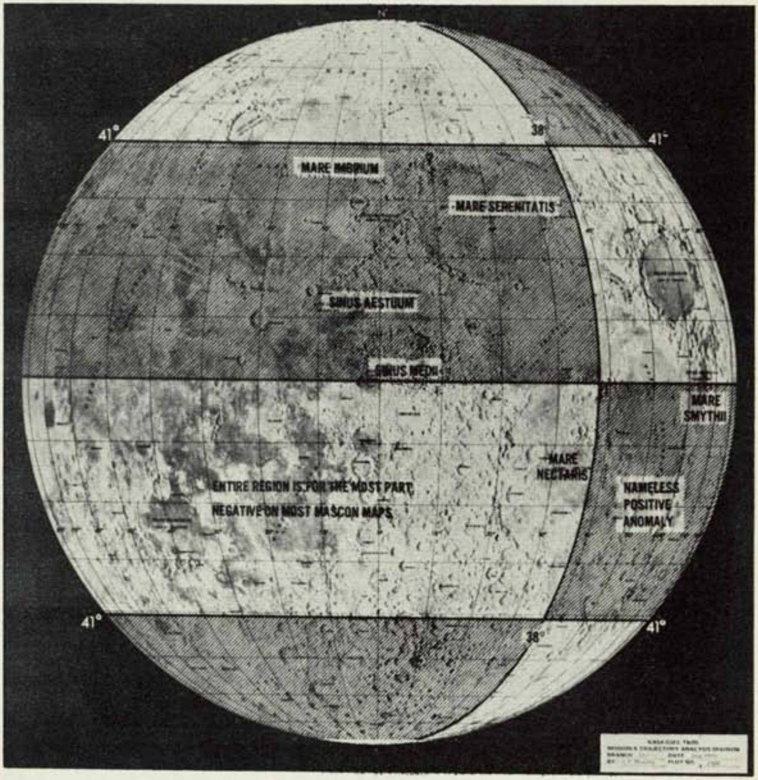

Figure 36—Gravitational effect of the (4, 1) coefficient in the ML1.1 field. (Note: Shaded areas correspond to positive anomalies)

End of Doc.